Preliminary design and analysis of a chassis side beam for stiffness and crashworthiness of an electric vehicle

José Pereira
jose.luis.pereira@tecnico.ulisboa.pt

Instituto Superior Técnico, Universidade de Lisboa, Portugal

November 2018

Abstract

Environmental concerns about combustion cars are pulling manufactures to build them electric. The majority of the electric car power cells are lithium-ion batteries. In the event of battery leakage, lithium can cause serious injuries on the passengers' body. Regarding side collisions, that represent 15% to 40% from all injury accidents, if only serious and fatal injuries are considered these values are increased by 50%. To protect passengers and batteries and also develop a component capable of integrating a chassis, this work focuses in the preliminary design and analysis of a chassis side beam for stiffness and crashworthiness. Taking into account the beam's function, a judicious choice of the aluminum alloy that will integrate it, is carried out. Two robust Finite Element Analysis (FEA) models are constructed, one that test the crash performance and another that certifies that the beam has the strength and stiffness enough to integrate the chassis. These models are inserted in a multi-objective optimization program based on a genetic algorithm. This program search for the best pole crash performance and the lightest beam, subjected to non-linear constraints. This tool will allow to obtain the optimized beam without losing engineering time in the iterative process of design and calculate. In this program, adaptive to new structures and purposes, several beams with different strategies were tested. Finally, a multi-thickness beam with a quadricular misaligned cross-sectional shape was chosen. This solution overcomes several project requirements and has the best commitment between pole crash performance and weight.

Keywords: multi-objective optimization, genetic algorithm, pole crash performance, stiffness

1. Introduction

Combustion cars have dominated for more than a century. However, environmental concerns about them are pulling and bringing new manufactures to build hybrid and electric cars.

With electric cars, new structural challenges will appear but the chassis will continue to be the integrating part of the vehicle frame that supports internal and external loads.

The majority of the electric car power cells are lithium-ion batteries. Their protection is of the utmost importance because, like all alkali metals, lithium is highly reactive and flammable and can cause side effects on the passengers' body like skin lesions and others [1]. For batteries protection and occupants safety, the efforts are focused on crashworthiness with the inclusion of parts strategically placed to absorb the maximum energy from an impact. One of these parts is the side beam chassis where this work have their center of attention. The tests on the modeled beam will be based on Finite Element Method (FEM), a method that overcomes the traditional variational methods [2].

This work is part of a larger project called Be2.0, a second version of the project Be developed by CEiiA. This is an on-demand vehicle for share use that can be driven by a human operator or autonomously. Powered 100% electric, this car will be a M1 class vehicle with Portuguese engineering from universities and several other entities partnerships.

The Be 2.0 follows the current strategy adopted by practically all electric car manufacturers of placing the batteries between axles and under the cabin. This strategy makes the side beam chassis a component with high requirements at structural level, because it not only needs to meet stiffness requirements but also is the connection between the rear and front modules of the car. Besides the structural requirements, this component must protect the batteries and occupants in case of lateral impact.

2. Background

2.1. Structural Principles

To evaluate if the beam has the necessary structural characteristics to integrate a car chassis, several in-

dicators are used. Stiffness and allowable stress are the most used structural principles to evaluate a chassis component.

Being the aluminum alloys a ductile materials, the Von Mises criterion interprets well the material yielding [3].This criterion computes the equivalent stress as

$$\sigma_{eq} = \sqrt{\frac{(\sigma_1 - \sigma_2)^2 + (\sigma_2 - \sigma_3)^2(\sigma_1 - \sigma_3)^2}{2}}. \quad (1)$$

where σ_1, σ_2 and σ_3 are the principal stresses. The yielding stress represented by σy is the point where the plastic deformation appear in the material. When σ_{eq} reaches the yielding stress the material starts to yield.

To maintain the structural integrity of the beam and security of the passengers, a 1.5 safety factor is normally used. This means that, in the worst load condition, the equivalent stress should not exceed 2/3 of the yield stress [4].

A chassis beam can be sufficiently strong but insufficiently rigid. Limits on the deflection and twist of the side beam chassis are very important to prevent problems in the response performance. The simple operation of closing and opening the door can be compromised if the side beam chassis is not rigid enough, or can even cause passenger insecurity if the car's floor is deflecting [4]. The rigidity of a beam is evaluated by the bending and torsional stiffness. The beam bending stiffness, or flexural rigidity, is the resistance against bending and can be evaluated by the product of the modules of elasticity E by the moment of inertia I [2]. Torsional stiffness is the resistance to twist and can be evaluated by the product of the shear modules G by the torsional constant J [5].

2.2. Crashworthiness Principles

To compare different beams and evaluate their crashworthiness performance, some indicators are used. The most common principles to evaluate crashworthiness are the energy absorption (EA), the average crash force (F_{avg}), the specific energy absorption (SEA), the peak crashing force (F_{max}) and the crash force efficiency (CFE) [6].

The energy absorption is defined by

$$EA = \int_0^{\delta} F(x)dx, \quad (2)$$

where $F(x)$ is the crash force and δ is the deformation. From which the average crash force can be found as

$$F_{avg} = \frac{EA}{\delta}, \quad (3)$$

and the specific energy absorption as

$$SEA = \frac{EA}{m}, \quad (4)$$

where m represent the mass of the beam. On the other hand, the peak crashing force is found from

$$F_{max} = Max(F(x)) \quad (5)$$

and the crash force efficiency is defined as

$$CFE = \frac{F_{avg}}{F_{max}}. \quad (6)$$

In crashworthiness performance, a high value of energy absorption with a low peak of force is desired, in other words, the goal is to absorb the maximum kinetic energy while maintaining a constant acceleration. This is evaluated by the CFE that needs to be as close to unity as possible [7].

2.3. Regulations

Before putting a car on the road, the manufactures need to fulfilled the government's impact testing requirements, to get the vehicle's homologation. United Nations Economic Commission for Europe (UNECE) is the regulation entity responsible for these tests in Europe.

Like UNECE, the European New Car Assessment Programme (Euro NCAP) performs crash tests, not to achieve vehicle's homologation but to help customers identifying the safest choice. The Euro NCAP is an independent association that performs more demanding tests like the side impact pole test. This test allows to simulate the event of the vehicle's lost control by the driver, followed by impact sideways into rigid roadside objects such as trees or poles [8]. This severe test consists of a sideways projected car against a rigid pole with a dummy placed in the driver's seat. Due to the localized impact, the pole intrusion in the car can be high and can cause serious injuries to the driver.

The impact must occur with the pole (a circular metallic rigid structure with 354±3mm in diameter) with a target speed of 32±0.5km/h. The car must impact the pole in the Impact Reference Line, that results from the intersection of the vehicle's exterior surface and a vertical plane, constructed by the passage through the head's dummy center of gravity and the intersection at 75° with the vehicle's longitudinal centerline [9].

The five-stars safety ranking was created by Euro NCAP where 5 stars represent overall very good performance in crash protection and 1 star represent marginal crash protection. In 2018, according to the Euro NCAP Rating Review [10], in the 5 star ranking, all tests are rated by summing 148 points The side pole test is included in the 38 points of Adult Occupant Protection. This test represents 8 points that are divided into 4 individual body regions: head, chest, abdomen and pelvis. There are several limits related to these body regions, however the most important ones for this work are the head capping limits:

- HIC_{15}<700;
- Peak resultant acceleration <80G;
- No direct head contact whit the pole.

2.4. Material Model

The side beam chassis needs to overcome not only structural but also crashworthiness requirements. In the structural analysis, the material elastic behavior is sufficient to design and to test it. In the crash analysis, the plastic behavior is fundamental because only with high deformations can we reach high absorbed energies from the impact.

For 3D problems, homogeneous and isotropic materials, the generalized Hook's Law describes the elastic material behavior. When the material reaches the yield point, the stress strain curve can be defined by the Johnson-Cook equation [11]. This equation is validated and very popular constitutive model to describe the material behavior under a high rate deformation processes,

$$\sigma = \left[A + B\left(\epsilon^{pl}\right)^{n}\right]\left[1 + Cln\left(\frac{\dot{\epsilon}^{pl}}{\dot{\epsilon}_0}\right)\right]\left[1 - \left(\frac{T - T_{room}}{T_{melt} - T_{room}}\right)^{m}\right], \quad (7)$$

where σ and ϵ^{pl} are the stress and plastic strain respectively; A, B, C, n and m are constants that are characteristics of the material; T, T_{room} and T_{melt} stands for the current, room and melt temperature respectively. The ratio $\frac{\dot{\epsilon}^{pl}}{\dot{\epsilon}_0}$ is the normalized plastic strain rate, where $\dot{\epsilon}^{pl}$ is the plastic strain rate and $\dot{\epsilon}_0$ is the reference plastic strain rate usually equal to $1s^{-1}$.

The influence of the relationship between stress and the plastic strain rate is only significant in deformations that are only observed in ballistic impacts, which is not the case. The temperature during the crash situation will be much smaller than the melting temperature, therefore the temperature dependence can be neglected [12].

In conclusion, the model can be expressed in a simpler form,

$$\sigma = A + B\left(\epsilon^{pl}\right)^{n}. \quad (8)$$

2.5. Optimization

All optimization methods can be divided into two major branches, the deterministic and heuristic ones. The most commonly used methods are the genetic algorithms and the gradient-based ones [13].

The gradient-based optimization algorithms are the most suitable for a large number of design variables. In a non-convex problem with multiple local minima, the solution obtained by gradient methods will be the local minimum nearest to the starting point. Another problem related to these algorithms is the assumption that the objective and constraints as smooth functions, which might not be the case [13].

Based on the theory of biological natural selection, the Genetic Algorithm (GA) is a method that search for a global minimum and is excellent to search in large and complex data sets. This method can solve not only constrained or unconstrained but also discontinuous, non-differentiable, stochastic or highly non-linear optimization problems [13] [14].

All things considered, in this work the optimization is based on the Genetic Algorithm.

The GA starts with a random initial group of candidates called individuals normally distributed throughout the domain, this group is called initial population. For each step of the method, a new population of individuals is created, or usually called, a new generation. In each generation, all individuals are tested against the objective function evaluating the their fitness. Following the evolutionary biology, the next generation is made based on elitism, mutation and crossover. This process is repeated creating successive generations until the stopping criterion is satisfied [14].

To formulate a multi-objective optimization problem (MOO), two or more objective functions are required that must be traded off in some way. If the objective functions are competing, there is no unique solution to the optimization, therefore, there are several optimal solutions that lie on the pareto front, that are non-dominated points. A point x dominates a point y if:

- The solution x is better than y in all objectives;
- The solution x is strictly better than y in at least one objective [15].

The solutions are compared based on their objective function values in the feasible space defined by the constraints on the MOO. The non-dominated solution is the one in which an improvement in one objective implies a degradation of another [14] [15].

When the results do not converge into a single solution, the evolutionary algorithm tries to find a set of solutions which lie on the pareto-optimal front and are diverse enough to represent the entire range of the pareto-optimal. The pareto-optimal front is the final pareto that the algorithm gives in the output when it reaches the stopping criteria. After the pareto-optimal front is found, choosing a single solution involves a higher-level information. The user needs to choose the best trade-off solution based on qualitative information.

In the present work, the *gamultiobj* a *MATLAB*® function that is based in the *NSGA-II* algorithm is used to find the pareto-optimal front [14] [15]. This function can be divided in five steps:

1. First each parent is selected by a tournament of individuals randomly chosen from the current population;

2. Create the child population from the selected parents by mutation and crossover;

3. Combine the current and the child population into an extended population;

4. Compute the rank and crowding distance for feasible individuals in the extended population;

5. Trim the extended population into the population size, this will be the next generation.

The *NSGA-II* algorithm can be summarized as demonstrates figure 1, where P_t represent the current population, Q_t the child population, R_t the extended population and the F_i the ranks.

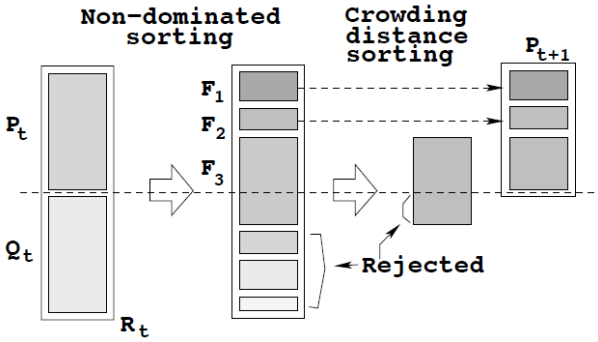

Figure 1: *NSGA-II* algorithm schematic (adapted from [15]).

In order to stop the algorithm, several stopping criteria can be used, but the most common are: maximum number of generations or function tolerance and a number of stall generations [14].

3. Implementation

The structure studied is highlighted in figure 2 where its position in relation to the Be2.0's chassis can be seen.

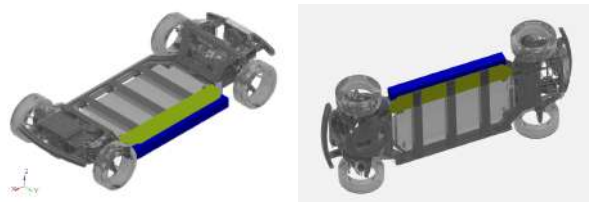

(a) Isometric View (b) Bottom View

Figure 2: Be2.0 chassis with the structure highlighted.

3.1. Project Requirements

The design of the side beam chassis for the Be2.0 is a rigorous process that has to meet dimensional, structural, crashworthiness, material and fabrication requirements, applied to the project by CEiiA.

The structural requirements are basically related with rigidity and stress. The maximum deflection in vertical direction of the beam must be less than or equal to 1mm, bearing 600kg uniformly distributed doubly supported at its tips in static and dynamic situation. The maximum torsional deflection must be less than or equal to 0.04rad, bearing 355.5Nm at its tips in static and dynamic situation. To simulate the worst case scenario, these two requirements must be computed simultaneously. The safety factor for the Von Mises criterion is 1.5. The beam must be constructed in an aluminum extrusion. The dimensional constraints are related with the batteries' height and with the length and width of the car. The beam's height must be 140mm and the length must be 1660mm (supported at 1600mm). To meet the Be2.0's total width the target value for the beam's width is 130mm.

The crahswortiness requirements are the most rigorous and difficult to overcome because the test applied to the beam must be as close as possible to the Euro NCAP pole test. The maximum acceleration, maximum HIC_{15}, velocity and pole dimensions must be equal to this test. The structure has to withstand the impact with 800kg and must ensure that the intrusion of the beam towards the interior of vehicle be less than 150mm. To perform a more demanding test than the Euro NCAP pole test on the analyzed values, in this test, the vehicle's motion forms an angle of 90º with the vehicle's longitudinal centerline.

3.2. Structural Analysis

During operation, the vehicle's chassis is subjected to various loading cases. The bending, torsion and the superposition of the two are the most important cases for the chassis analysis. The lateral, fore and aft loading are very important to other studies like suspension performance.

The dynamic bending loading that appears during the car operation must be considered, not only due to force peaks, but also due to fatigue failure. Experience in car manufacturing allows a simplification of the dynamic analysis, consisting of just increasing the static loads by 2.5 times and make the study in static behavior. These multipliers are called dynamic factors [4].

During the car operation, pure torsion on the chassis is very unlikely to happen, it appears always combined with vertical load. The maximum torsion moment takes place when one wheel from the less loaded axle is raised until the opposite wheel leaves

the ground. Again to simulate the dynamic effect, a dynamic factor of 1.3 is used [4].

3.3. Aluminum Alloy Choice

To choose the aluminum alloy that meets all requirements, it is imperative to analyze various aspects. The strategy is to first select the alloys that fulfill the restricted requirements like corrosion resistance, weldability and extrusion, and then among the selects ones, choose the one that has the best structural and crashworthiness performance.

The 6xxx alloy series present the best commitment between corrosion resistance, weldability and extrusion. The alloys from this series with less than 200MPa tensile yield strength were not analyzed in structural and crashworthiness performance.

The shear modulus G, elastic modulus E and density ρ present a small variation among the 6xxx alloys. The values that present a considerable variance are the ultimate resilience (that measures the amount of energy absorbed by the material until its fail, one of the most important parameters in crashworthiness performance), the shear and yield strength. Therefore, the choice is going to be based in the best commitment of these three parameters. Graphically, this comparative can be observed in figure 3.

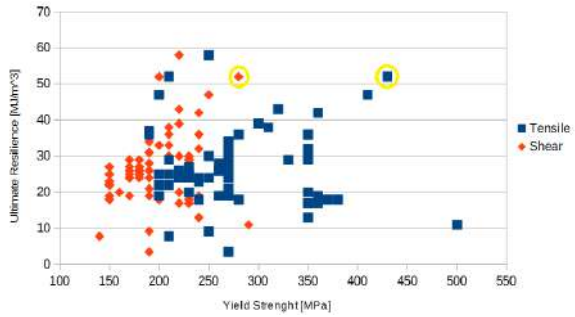

Figure 3: Ultimate resilience vs tensile and shear yield strength

The alloy marked with yellow circles in figure 3 is the 6110A-T6 alloy. This alloy maximize the relation between ultimate resilience, tensile and shear yield strength. It is normally used in bumper systems, crash management systems and side sills [16].

3.4. Optimization Cycle

To design the beam, an optimization cycle fully controlled by a *MATLAB*® program was created as schematically show in 4.

The *MATLAB*® program controls the overall process giving the inputs to the cycle, and then, receiving and analyzing the outputs. Cycle inputs are the variables to be optimized in the beam which can be for example width, thickness, reinforcements or even material. Everything that is parameterizable in *CATIA*^{TM} *V5*, or even parameters in the *HYPERMESH*®, can be variables of the cycle, giving a huge freedom to the user to choose what to optimize.

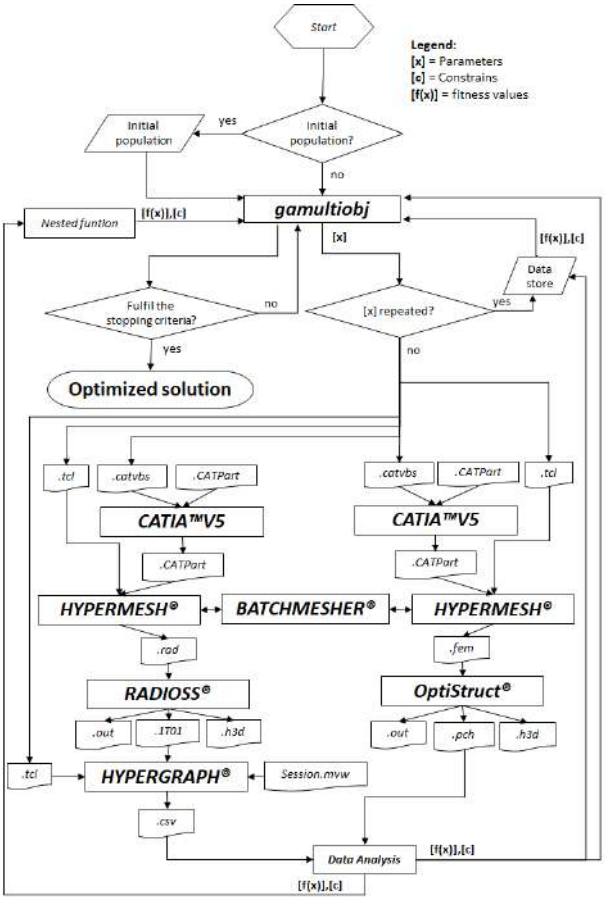

Figure 4: Optimization cycle schematic

The *MATLAB*® program is where the genetic algorithm is implemented. This algorithm is found in functions from the *MATLAB*® library, in which, for multi-objective problems, the *gamultiobj* function is used in this work. The *gamultiobj* finds a local pareto front for multiple objective functions.

Since the objective of this project is to increase the performance of the beam in crash, as well as to reduce its mass the objective functions are 1/CFE and the beam's mass. The results from the objective functions depend on the realized simulations in this cycle, as well as the constraints: HIC_{15} $\leq$700, acceleration $\leq$80G, intrusion $\leq$150mm, torsional deflection $\leq$0.04rad, displacement in vertical direction $\leq$1mm and Von Mises equivalent stress $\leq$322.5MPa. These constraints depend on the computational simulations, therefore they are considered non-linear. All this cycle is inserted into a single function that is invoked by the genetic algorithm. This drags an associated problem, both the

objective functions and the non-linear constraints depend on the same function. The time consumed at each iteration is the main problem of this cycle and, to avoid the cycle being invoked twice in a single iteration, it was created an embed function in nested function. These functions keep recent values to calculate the constraints and the objective functions just once. This function, once called the cycle function to calculate the objectives or the non-linear constraints, calculates both and saves the results. When it is called again only returns the results previously calculated [14].

The same strategy is used to avoid calculate the individuals previously calculated in the same or previous generations. The results of all individuals are saved in a matrix inside the cycle function. The elite individuals that go into the next generation, or even repeated individuals formed by crossover or mutation, are calculated just once allowing a large time savings.

The control of the other programs is also done by the *MATLAB*® script. All programs run with their respective macros from the *Windows* command line. This is possible with the help of the *dos* function that executes the specified *Microsoft*® Disk Operating System (MS-DOS) command for *Windows* platforms.

The optimization cycle is divided into two main branches, the crash simulation and static simulation branch. The first step in both branches, is to create a CAD3D model parametrized in the variables that we intend to optimize. In the branch of the static simulation, this file contains only the beam. In the branch of crash simulation, this model contains the beam plus the auxiliary structures, to better simulate the connections and how the forces propagate when the beam hits the pole. In both simulations, a macro (*.catvbs*) is created to perform the necessary changes, save them, and export a *.CADPart* file.

The *HYPERMESH*® program is responsible for the pre-processing the numerical models. This program receives the file exported by *CATIA*™ *V5* and performs all the necessary operations such as boundary conditions, mesh creation , load cases etc. The *BATCHMESHER*® program is used to create the mesh. This program is invoked during the implementation of the *HYPERMESH* macro and it creates the mesh for both models with the element size according to the respective mesh convergence study. In both simulations, all the steps performed in *HYPERMESH*® are made following their respective macro (*.tcl*). This macro is changed at each iteration of the cycle to make the pre-processing process adapted to the analyzed beam. When the pre-processing of the models is finished, two files with the respective models are exported. The solvers *RADIOSS*® and *OptiStruct*® receive these files and run the crash and static numerical models respectively.

The *.pch* file is the output of the *OptiStruct*® solver. Since this file is readable by *MATLAB*® functions, it is possible to carry out the data post-processing directly on it. Here, the maximum deflection in vertical direction, the maximum torsion along X-axis (longitudinal) and the maximum Von Mises equivalent stress are evaluated.

The *.T01* file is the output of the *RADIOSS*® solver. Since this file is not readable by *MATLAB*® functions, another program is needed to export a file that allows this reading. The *HYPERGRAPH*® is the program that receives the *.T01* file and exports the important data of this analysis into a *.csv* file. To perform this operation, it is necessary to create a session file that contains the information about what to export. Finally, we need to create a macro that applies this session, save and export the data into a *.csv* file. From this file, it is possible to calculate the results of the objective functions and the remaining constraints (HIC_{15}, acceleration and intrusion).

The results are stored in a matrix and returned to the genetic algorithm that performs this process iteratively until the stop criterion is satisfied.

4. Experimental Study and Validation

Due to lack of equipment, material and resources, these experimental validations were not done. However, this section discusses how the experimental tests should be performed.

4.1. Material Model Validation

Before testing the whole structure in a laboratory, it is important to make sure if the materials used in these tests have the correspondent behavior of the material modeled in the computational material model. With material samples from the same materials that will be used to construct the components of the structure, it is possible to perform tensile tests. These tests can validate if the structure is being constructed according to what was designed computationally. The two aluminum alloys used in this project must be tested in this experimental study (beam 6110A-T6, axillary structures 6061-T6). To test the samples, we need a machine. The universal testers are the machines most used to perform this type of tests. Specialized in obtaining stress-strain curves, these hydraulic machines are based on a piston that moves the crosshead up or down. This machine read the tensile force as function of the increase gage length, therefore, to obtain the stress-strain curve we must normalize the data with respect to the sample dimensions. In other to obtain more accurate results, it is important to test several samples of each material, and with these data, calculate a weighted average of all

stress-strain curves for each material [17].

4.2. Crash Model Validation

To validate the crash numerical model, first we need to construct the structure.

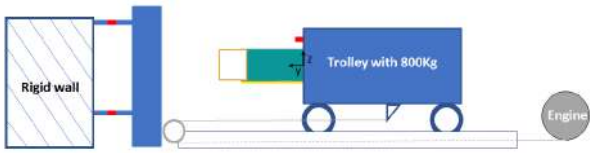

Figure 5: Experimental crash test layout.

It is very important that the activation, the monitoring and the data collection be performed fully automatic to not have people near the structure at the impact moment and thus, execute the laboratory test safely.

We need a trolley with a mass of 800Kg. The front of the trolley must be welded with the structure. The center of gravity of the trolley must be aligned with the plane $x = 0$, in an effort not to produce unwanted moments. The trolley moves in two rails, with this strategy, the trolley will just move in the Y direction.

The traction system is composed by an electric motor, a pulley and a cable. The position layout of these components are shown in figure 5. The impact must occur with a target speed of 32±0.5km/h. At the instant before the collision with the pole, the motor must be automatically switched off.

The pole is a circular metallic rigid structure with 354±3mm in diameter. We must have 6 load sensors on the pole's supports. The force-time curve will be calculated by summing the contributions of each sensor in the Y direction. This curve must be filtered according SAE J211. Finally, we can merge the force-time curve with the displacement-time curve and get the force-displacement curve. To validate the computational model, the experimental and the computation curves must be approximately equals.

4.3. Static Model Validation

Due to the early stage development of the Be2.0, the load application points of the cabin in the beam are not yet known. Therefore, a pressure was applied throughout the upper part of the beam to simulate the bending effect, that it would be subjected during vehicle's operation. To simulate the worst case scenario, in the previous model the maximum moment that the beam has to support was applied, to contribute to the global torsional stiffness of Be2.0. These two combined loads became somewhat complicated to simulate in a laboratory. Virgínia Infante, university teacher at Técnico Lisboa from the scientific area of mechanical design and structural materials and specialist in materials laboratory, affirms that such experimental test is not possible to perform in a laboratory [18].

5. Results

Five optimizations with different strategies and cross-sectional shape beams were preformed as demonstrated in figure 6:

- Optimization 1 - Rectangular Shape;
- Optimization 2 - Aligned Quadricular Shape;
- Optimization 3 - Misaligned Quadricular Shape;
- Optimization 4 - Aligned Quadricular Shape With the First Width Division Thicker;
- Optimization 5 - Misaligned Quadricular Shape With the First Width Division Thicker.

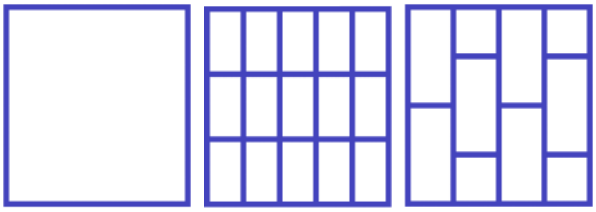

(a) Rectangular (b) Aligned Quadricular (c) Misaligned Quadricular

Figure 6: Different beam's cross-sectional shapes.

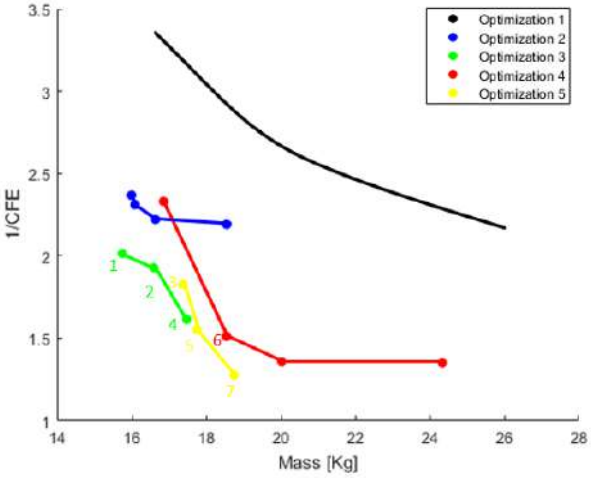

Figure 7: Pareto fronts of the five optimizations.

Only integer variables were allowed in the optimizations 2, 3, 4, and 5. These strategy allows to optimize the number of divisions and reduces the search area. In this optimizations, an initial population of individuals was given to the genetic algorithm. These individuals were chosen based on the

sensitivity of the programmer to know where the best solutions may be found. This strategy permits a faster convergence of the method.

The first optimization performed in this project was to test the method. The beam width was allowed to change and to be optimized. The beams with higher widths have an advantage in relation to the narrower beams because they allow a greater displacement with less intrusion. At the end of this optimization, it was concluded that the intrusion would be the constraint that would reprove more individuals. It can also be concluded, that the CFE increase is only achieved by increasing the mass, proving the competitiveness between the objective functions. In this optimization, individuals that fulfilled all the constraints were obtained, however presented mediocre crash performance. The lightest beam that was able to overcome all constraints, obtained in this optimization has a mass of 16.54kg. On the other hand, the beam with the best crash performance has a CFE of 0.464 but presents a mass increase of 57.9%, in relation to the lightest beam.

Since optimization 1 onwards, all optimizations were performed following the strategy that a higher deformation in the beam would lead to a higher energy absorption in a lower displacement. A smaller displacement will lead to less intrusion. On the other hand, a higher deformation in the beam width zone will lead to a higher displacement, without this implying a same magnitude increase in the intrusion of the beam towards the interior of the vehicle.

The implemented strategy was a success in optimization 2, the quadricular shaped beam led to an increase of the CFE to any corresponding value of mass in optimization 1. Therefore, the individuals from optimization 2 dominate almost all optimization 1 individuals. However, the improvements obtained in the optimization 2 were insufficient. The pareto front individuals of this optimization still present a high peak force in relation to the average force, the individual with the best performance in crash presents only a CFE of 0.456.

With the objective of decreasing the peak force and obtaining more deformation in the beam width zone, the strategy of having a quadricular shape beam with the squares misaligned half their size was implemented in optimization 3. In this optimization the lightest beam (15.75kg) that can overcome all constraints among all optimizations was obtained. In addition to be the lightest, this individual has a CFE of 0.497. Better than any CFE presented in optimization 2, therefore, this individual dominates all individuals from optimization 2. In this optimization it was found the best CFE so far, the individual presents a CFE of 0.619 for a mass of 17,48kg. Simply by increasing its mass by 11%, the CFE was raised by 25%, when compared to the lightest beam.

Not satisfied, and with the objective of improving the beam and adding value to the project, a new strategy was implemented in the existing beam shapes. The strategy was to set the thickness of the first beam width division different from the rest of the divisions. This second thickness became another parameter to be optimized and was forced to be thicker than the rest of the beam. The strategy was to place the smaller thickness divisions in contact with the pole in order to deform this part of beam more easily and, consequently, reduce the initial peak force. The larger thickness is placed in the first beam width division to increase the force after the peak, in an effort to increase the CFE. This larger thickness division acts as a "barrier" to intrusion and give the sufficient stiffness in the static test.

In optimization 4, this strategy was applied to the aligned quadricular shape beam. As we can see there was an improvement in CFE in relation to the same beam without this applied strategy (optimization 2). This improvement was always followed by a mass increase. The lighter individual found in this optimization is dominated by the optimization 2 individuals.

In optimization 5, it was applied this strategy to the misaligned quadricular shape beam. Comparing to optimization 4, the same behaviour was observed in the results. The improvement in crash performance was always followed by a mass increase relative to optimization 3 individuals.

We can conclude by comparing the pareto fronts from the optimization 2 and 3 and from optimization 4 and 5 that the beams with the misaligned quandricular shape dominate almost all aligned quandricular shape ones. It is possible to conclude, as well, that the strategy of forcing the first beam width division to be thicker always presented heavier results. However, with a substantial improvement in crash performance comparing aligned with aligned quadricular shape beams and misaligned with misaligned quadricular shaped beams.

The non-dominated individuals are numbered in figure 7 from 1 to 7. If the objective was to obtain the lightest beam or the highest CFE we should choose the beam 1 or 7 respectively. But the goal here is obtain the best balance between the two objective functions. Therefore the final solution will be the beam 2, 3, 4, 5 or 6.

Although individual 2 (CFE=0.519, mass=16.60kg) is 6.5% lighter than individual 4 (CFE=0.619, mass=17.48Kg), if we compare the crash performance, individual 4 presents an increase in CFE of about 19%. The same happens with individual 3 (CFE=0.548 mass=17.38kg). For almost the same mass, individual 4 presents an

increase in CFE of about 11.5%. Individual 4 is also less intrusive than individuals 2 and 3.

If we compare individual 5 (CFE=0.644, mass=17.75kg) with the individual 6 (CFE=0.661, mass=18.55kg), we notice that individual 6 presents an increase of 2.6% in CFE. But this improvement is just achieved by increasing its mass by 4.5%. In addition, individual 5 is less intrusive than individual 6. This leave us with two options, individual 4 or 5. Individual 5 presents an increase of about 4% in the CFE with just increasing its mass by 1.5% in relation to the individual 4. But the major difference between them is the maximum acceleration, individual 5 presents 23% less maximum acceleration than individual 4.

All things considered, the beam 5 is the chosen one: a quadricular shape beam with the squares misaligned and with the strategy of forcing the first width division to be thicker than the rest of the beam. It is formed by 2 divisions in height, 6 in width, thickness1 with 2mm and thickness2 with 5mm.

Figures 8, 9 and 10 were all computed from the performed simulations on the chosen beam. Figure 8 shows the static test result, where the displacement in Z direction is measured for all nodes, presenting lower values than 1mm.

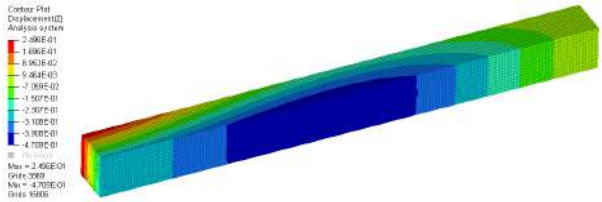

Figure 8: Displacements in vertical direction - static test.

In figure 9, the curve force-displacement is represented with the maximum and average force evidenced where the proximity between the two forces can be observed. It can be concluded that this curve matches the optimal curve in crashworthiness, low peak force and the area below the curve maximized.

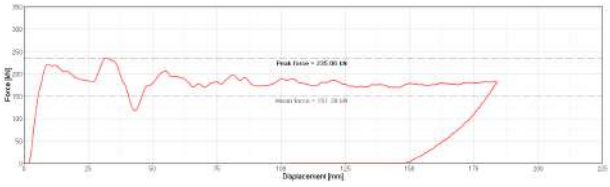

Figure 9: Force-displacement curve of the chosen beam.

Figure 10 shows the result of the crash pole test evidencing the differences between before and after the collision.

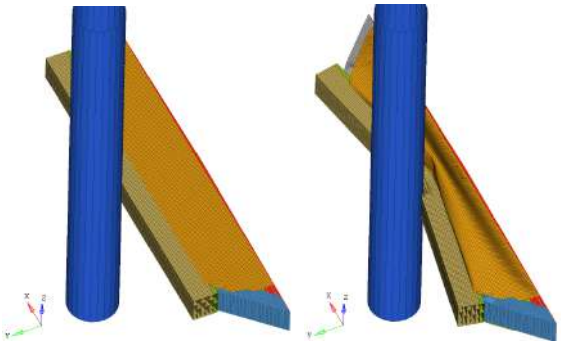

(a) Before. (b) After.

Figure 10: Pole test results on the chosen beam.

6. Conclusions

The main objective of this project was to design a side beam chassis that must fulfill requirements of stiffness and crashworthiness. To develop it, two robust numerical models were created, inserted in a multi-objective optimization program based on a genetic algorithm. This program searches for the best pole crash performance and the lightest beam, subject to non-linear constraints (HIC_{15}, acceleration, intrusion, torsional deflection, displacement in vertical direction and Von Mises equivalent stress.).

This chassis will have new applications such as smaller or larger cars, mini buses or cargo vehicles. For this reason, it was very important to develop a powerful and flexible tool that can easily redesign and recalculate a new beam for other applications. This resizing can be achieved by only changing the input parameters of the optimization cycle such as mass, width, height, material, etc.

In order to add value to this work, and simultaneously to develop an optimized beam for this vehicle, several beam shapes and strategies were implemented. The implementation of quadricular shape beams, with squares aligned or misaligned, as well as the strategy of forcing the first width division to be thicker than the rest of the beam, proved to be a success. The results were obtained with increasingly better crash performance with lighter beams.

6.1. Deliverables and Achievements

The major deliverables were:

- Multi-objective optimization program based on a genetic algorithm, which automatically returns an optimized beam;
- A versatile optimization program that allows to change the objective functions, dimensions, beam shapes, materials, parameters to optimize and others, was developed;
- Two robust numerical models were build, a non-linear explicit and a linear static;

- A database that allows evaluation of how the different types of beam shapes behave and how the optimized parameters influence this behavior.

The major achievements included:

- An optimized beam for application in Be2.0 that fulfills all project requirements, such as materials, fabrication, dimensions, stiffness and crashworthiness. This design structure meets the initial goals from the Euro NCAP pole test;

- Beams with quadricular aligned and misaligned shapes allowed for lighter structures with better crash performance, than beams only composed by one rectangle;

- The implemented multi-thickness strategy, forcing the first width division to be thicker than the rest of the beam, proved to be beneficial in crash performance;

- The single thickness strategy allowed for lighter beams than the multi-thickness strategy;

- Beams with quadricular misaligned shape allowed for lighter structures and with better crash performance, than beams only composed by a quadricular aligned shape.

References

[1] Michael Gitlin. Lithium side effects and toxicity: prevalence and management strategies. *International Journal of Bipolar Disorders*, 4(1):27, 2016.

[2] J. N. Reddy. *An Introduction to Finite Element Method*. R.R. Donnelley & Sons Company, 2^{nd} edition, 1993.

[3] Walter D. Pilkey and Deborah F. Pilkey. *Peterson's Stress Concentration Factors*. John Wiley & Sons, 3^{nd} edition, 2008.

[4] Julian Happian-Smith. *An Introduction to Modern Vehicle Design*. Butterworth-Heinemann, 1^{nd} edition, 2002.

[5] A. F. Hughes, D. C. Iles, and A.S. Malik. *Design of Steel Beams in Torsion*. The Steel Construction Institute, 2011.

[6] Tao Tang, Weigang Zhang, Hanfeng Yin, and Han Wang State. Crushing analysis of thin-walled beams with various section geometries under lateral impact. *Thin-Walled Structures journal*, 102:43–57, 2016.

[7] Pedro Gomes Mota Rebelo. Design study of a side intrusion beam for automotive safety. Master's thesis, Instituto Superior Técnico, Portugal, 2016.

[8] European New Car Assessment Programme - Side Pole. `https://www.euroncap.com/en/vehicle-safety/the-ratings-explained/adult-occupant-protection/side-pole/`. [Accessed July 2018].

[9] European New Car Assessment Programme - Side Pole. Oblique Pole Side Impact Testing Protocol, 2017.

[10] European New Car Assessment Programme - Side Pole. Euro NCAP Rating Review 2018, 2018.

[11] M. Grazka, J. Janiszewski, L. Kruszka, E. Cadontand D. Forni, and G. Riganti. Identification methods of parameters for johnson-cook constitutive equation – comparison. *Applied Mechanics and Materials*, 566:97–103, 2014.

[12] Tiago Miguel Encarnação Nunes. Multi-objective design optimization of a frontal crash energy absorption system for a road-safe vehicle. Master's thesis, Instituto Superior Técnico, Portugal, 2017.

[13] André C. Marta. Aircraft optimal design - MSc course notes. Instituto Superior Técnico, Portugal, 2015.

[14] MathWorks. MathWork help. `https://www.mathworks.com/help`. [Accessed July 2018].

[15] Kalyanmoy Deb. Multi-objective optimization using evolutionary algorithms: An introduction. Indian Institute of Technology Kanpur, India, 2011.

[16] HYDRO. HS6110 alloy. `https://www.hydroextrusions.com/en-US/why-aluminum/the-material/the-right-alloy/hs6110-alloy/`. [Accessed March 2018].

[17] J.R. Davis, editor. *Tensile Testing*. ASM International, 2^{nd} edition, 2004.

[18] Virgínia Infante. Private conversation, Instituto Superior Técnico, Portugal. September 2018.